MICROACOUSTIC TECHNIQUES TO ASSESS TO LOCAL CHARACTERISTICS OF IRRADIATED FUEL MATERIALS

B. CROS*[1], D. BARON[2], V. ROQUE[1]

[1] LAIN, Université Montpellier 2, 34095 Montpellier Cedex 05, France
[2] EDF, Division Recherches et Développements, 77250 Moret/Loing, France

The thermomechanical analysis of PCMI (Pellet to Clad Mechanical Interaction) failure risk is one of the major concern when designing the nuclear fuel rod. Code simulations are used for such analysis. The accuracy of the simulations requests a correct evaluation of the local properties of the materials. Improvement are still needed in the local characterisation of high burn-up fuel materials. Aiming this target, microacoustic techniques have been developed to perform local characterisations of the elastic properties on fuel materials, and of the pore volume fraction as well. A single set-up adapted to operate in hot cell by two complementary techniques, acoustic microscopy and microechography, has been designed. Working at 15 MHz, acoustic microscopy provides local measurements of the Rayleigh velocity through the study of the acoustic signature. Microechography used at a 40 MHz frequency give access to the longitudinal velocity. The local elastic constants and the relative pore volume can be deduced from the Rayleigh and the longitudinal velocities.

INTRODUCTION

The knowledge of the alteration of the mechanical properties of nuclear fuel pellets with burn-up is needed when simulating the fuel rod thermomechanical behaviour to demonstrate the integrity of the zircaloy cladding all along the fuel rod life, mainly during fast transient operating conditions. The classical characterisation techniques, neither static methods like uniaxial compressive mechanical tests, nor dynamical methods like resonance frequency measurements, cannot be used because of the fragmentation of the pellets. Moreover as burn-up proceeds, a radial gradient of modifications is observed depending on the local fission density, the local accumulated burn-up and the local temperature history, which allow or not irradiation defect recovery. Therefore, only local measurements can characterise properly the irradiated material. In fact, the main mechanical changes involve the rim region [1] where matrix Xe depletion, pore formation and local grain subdivision around pores are observed [2]. These changes result in a lower thermal conductivity of the rim zone [3] (due to a larger porosity and the fission product content [4]) and the elevation of the fuel temperature [5].

Characterisation of the porosity build-up is at present obtained by an automatic image analysis performed on high magnification optical ceramography or on SEM pictures. One knows how operator dependant are these evaluations. Providing this kind of measurement with an alternative method would then be welcome.

---

* Corresponding author. E-mail cros@lain.univ-montp2.fr

Two complementary methods are nearly available to measure locally the fuel material mechanical properties. They are based on the micro-indentation and the microacoustic techniques. In fact, the elastic constants can be deduced from ultrasonic velocity measurements and the echography has been used to characterise polycrystallized uranium dioxide [6] as well as single crystals [7]. Nevertheless, on the one hand this technique gives an overall information on the sample properties, on the other hand it cannot be used on fractured materials because of the large area covered by the beam. The aim of this work is to present the capabilities of the microacoustic techniques, acoustic microscopy and microechography. Measurements are carried out on non-irradiated pellets, but the set-up is designed to be driven in a hot cell.

THE MICROACOUSTIC TECHNIQUES

Microechography

Echography is used in industrial and medical fields for non-destructive testing and non-intrusive imaging. The originality of the high frequency microechography lies in the use of small size sensors which investigate limited areas. It consists in measuring the time interval between two echoes reflected by the parallel faces of a plate shape sample. The local longitudinal velocity V_L can be calculated in this way. The aperture angle of the lens is designed so that the beam can be regarded as slightly focalised in the investigated area. The longitudinal size of the spot should be larger than the sample thickness (fig. 1). The lens diameter should be as low as possible, but cannot be smaller than some wavelengths to save a diffraction phenomena enhancement.

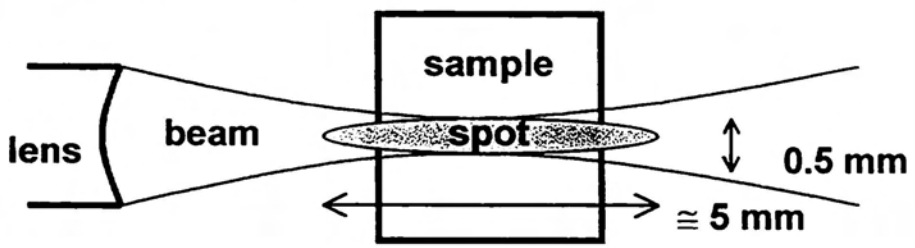

Fig. 1 – Shape of the focal spot in microechography.

Acoustic microscopy

Acoustic microscopy operates in the frequency range from some MHz to 1 GHz. This technique differs from microechography for the use of a beam focused by a spherical lens (fig. 2), which provides good lateral and longitudinal resolution. Resolution is closely related to the microscope working frequency, which is chosen according to the size of the investigated structure.

Acoustic microscopy operates through two complementary modes, imaging and acoustic signature [8,9]. In imaging mode, local mappings of the elastic properties of the sample are drawn up by scanning. Acoustic signature processing provides quantitative information on microvolumes which can be limited to some thousands of μm^3 by using high frequencies like 1 GHz.

Acoustical imaging

Images are obtained by scanning the sample in a *xy* plane perpendicular to the sensor axis. They are called "surface and sub-surface" or "bulk" images, depending on the beam focusing, whether on the surface, or in the depth of the sample. The Rayleigh wave, whose role in imaging is the most significant, penetrates in the material with a depth of about a wavelength before back radiating towards the lens. When the sample roughness is less than one wavelength, images are mappings representative of changes in elastic properties or, more exactly, of changes in the product $\rho.V_R$, ρ being the density of the sample material and V_R the velocity of the Rayleigh mode of the acoustic waves.

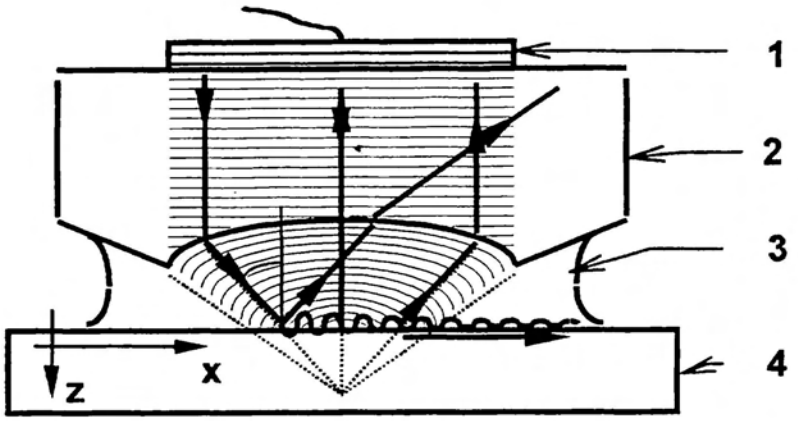

Fig. 2 – Coupling between the microscope sensor and the sample.
1- Piezo-electric transducer. 2- Delay line. 3- Couplant. 4- Sample.

As well as optical or electronic microscopy, high frequency scanning acoustic microscopy requires a surface dressing by polishing which generates additional defects. The observed porosity can have been created or modified by the polishing stage. Acoustic microscopy can offer advantage only if it provides resolution of the same order as optical microscopy and, especially, if sub-surface and bulk images, less dependent on polishing effect, can be obtained.

Acoustic signature

Acoustic signature $V(z)$ is obtained by varying the distance z between lens and sample. The signal transmitted back to the sensor is the result of interferences between the incident waves and the surface waves (fig. 2). Its variation as a function of z is pseudo-periodic and damped down. The velocity of the Rayleigh waves and, in some cases, of the longitudinal waves can be deduced through the $V(z)$ curve with an accuracy of about 1 $^0/_{00}$ from the relation

$$V = V_f[1 - (1 - V_0/2f\Delta z)^2]^{1/2} \qquad (1)$$

where V_f is the velocity in the coupling fluid, f the operating frequency and Δz the period of the pseudo-oscillations. The velocities V_R, V_L and V_T of the Rayleigh, the longitudinal and the transverse mode are related by

$$4\,(V_T/V_R)^{1/2}(1 - V_T^2/V_R^2)^{1/2}\,(V_T^2/V_L^2 - V_T^2/V_R^2)^{1/2} + (1 - 2\,V_T^2/V_R^2)^{1/2} = (\rho_0/\rho_S)\,(V_T^2/V_L^2 - V_T^2/V_R^2)\,/\,(V_T^2/V_0^2 - V_T^2/V_R^2)^{1/2} \qquad (2).$$

The surface waves being very sensitive to the properties of the sample, the $V(z)$ response can give valuable information about local changes in the material constitution.

Couplant choice

High frequency acoustic waves do not propagate in air. Coupling between lens and sample (fig. 2) is ensured by a liquid, whose properties govern the characteristics of propagation and back radiation of the waves. The choice of the couplant characteristics is related to the nature (metallic or ceramic) of phases constituting the sample and to its microstructure. The criteria differ depending on the operating mode, whether it be imaging or local measurement. The couplant interferes according to its acoustic parameters, velocity and attenuation of the longitudinal waves and density. Water is commonly used as couplant. Its chemical reactivity is weak and its attenuation remain low enough. The resolution of acoustic microscopes is improved by using high frequencies, but limited by the couplant attenuation which increases with the frequency square. As a consequence, the choice of frequency results from a compromise between resolution and attenuation. At very high frequencies, aqueous solutions of electrolytes are suitable couplants [10]. Their attenuation is weaker than water attenuation and their acoustic characteristics – velocity and density – can be adjusted according to the choice of nature and concentration of solvated ions.

Mechanical constant calculation

The mechanical features, Young modulus E, shear modulus G and Poisson's coefficient ν, as well as the Debye temperature Θ_D can be calculated from the measurement of V_L and V_T, the velocities of the longitudinal and transverse waves and from the knowledge of the density ρ :

$$E = [3 - 4 (V_T/V_L)^2] / [1 - (V_T/V_L)^2] \rho V_T^2 \quad (3) \qquad G = \rho V_T^2 \quad (4)$$

$$\nu = [2 (V_T/V_L)^2 - 1] / 2 [(V_T/V_L)^2 - 1] \rho V_T^2 \quad (5)$$

$\Theta_D = h.\nu_D / k$ where h is the Planck constant, k the Boltzman constant, ν_D being calculated from : $\nu_D = [9N / 4\pi a^3 (1/V_L^3 + 2/V_T^3)]^{1/3}$

where N is the number of atoms in a unit cell and a the lattice parameter of the compound. The Debye temperature is an indication of the shape of the potential energy.

The transverse velocity V_T can be calculated from V_L and V_R by (2). If only V_R can be deduced from the acoustic signature, V_L should be determined by microechography measurements.

EXPERIMENTAL SET-UP

Apparatus

In order to optimise the experimental setup, acoustic microscopy studies have been carried out, some of them in hot cell [11], at various frequencies, namely 15, 50, 130, 570 and 980 MHz. They have led to develop an original setting to characterise irradiated fuel materials. This equipment is adapted to work in hot cell at the Institute for Transuranium elements in Karlsruhe. It is made of an acoustic microscope operating at 15 MHz and a microechograph working at 40 MHz. In fact, because of the high density of the sample material, the efficiency of the back-radiated acoustic modes is weak and the acoustic signatures recorded at frequencies higher than 15 MHz are not exploitable. Moreover, at this frequency, the only Rayleigh velocity can be accurately measured (fig. 3). The longitudinal velocity needed to calculate the shear velocity and the elastic constants through relations (3-5) should be measured by microechography.

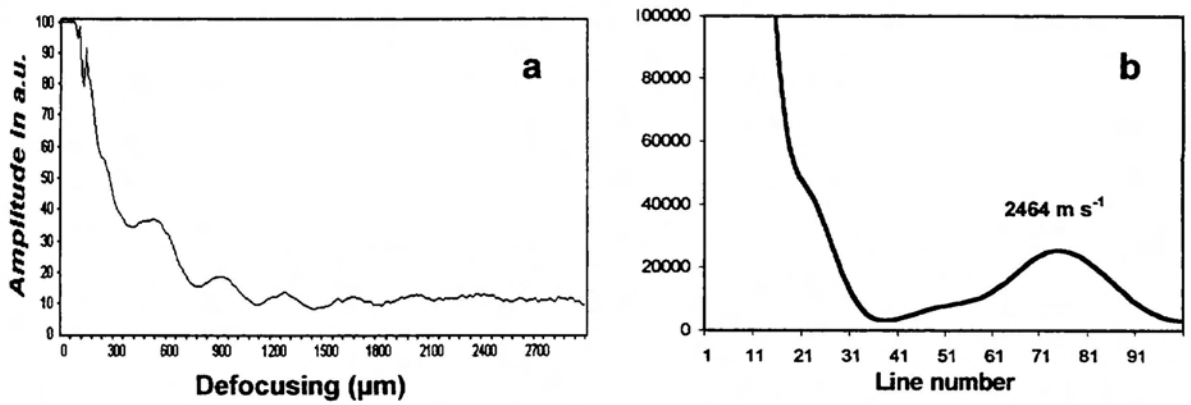

Fig. 3 – Acoustic signature acquired at 15 MHz on an UO_2 pellet (a) and FFT treated spectrum (b).

Resolution

To be well adapted to the characterisation of the mechanical properties of strongly irradiated pellets, the developed methods should have a sufficient resolution to reveal a radial gradient and to carry out measurements on fragmented samples. The sensor adapted to record acoustic signatures at 15 MHz is designed with a 50° aperture angle. When the beam is focused on the sample surface, the spot diameter is about $\lambda/2$, then roughly 50 µm. During the sensor moving toward the sample for *V(z)* recording, the spot diameter is enlarged to reach 1200 µm for a 1500 µm defocus and 2400 µm for the final 3000 µm defocus. To evaluate the area investigated by the local measurement, the energy concentration at the center part of the scanned area should be taken into account. Therefore, the diameter of the investigated area can be estimated to be around 600 and 1200 µm for 1500 and 3000 µm defocus respectively.

The sensor designed for microechography measurements generates a slight defocused beam (some degrees) to compensate the divergence due to the diffraction and the spot diameter is around 500 µm (fig. 1).

EXPERIMENTAL STUDIES

Acoustical imaging

Images have been obtained at high (570 MHz) and very high (980 MHz) frequencies thanks to the choice of very few attenuating couplants, like aqueous solutions of electrolytes. They clearly reveal the porosity (fig. 4, 5 and 6a), but remain analogous to optic images (fig. 6b) because they characterise the sample surface and not the bulk. In fact, owing to the very high density of the fuel materials, the acoustic beam is strongly reflected. The penetration of the beam in the bulk can be improved by a couplant whose density is closer to the one of the sample, hence a liquid metal. Bulk images have been obtained using mercury as couplant and a sensor with a small aperture angle to suppress the surface waves. Although they are rich in contrasts (fig. 6c), they are not exploitable without an adapted image processing.

Fig. 4 – Acoustic image at 930 MHz near the surface of a non-irradiated fuel pellet.

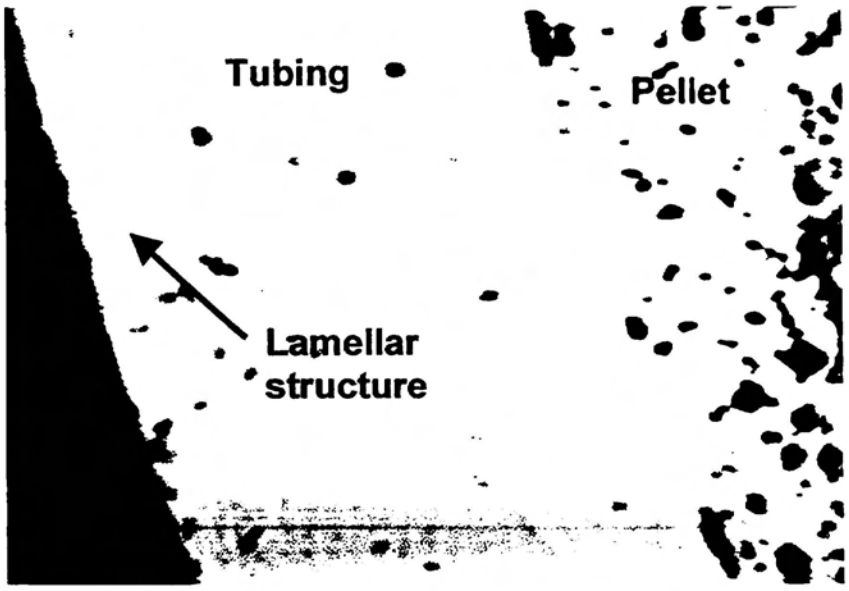

Fig. 5 – Acoustic image at 130 MHz of the cross-section of the pellet and the tubing after 5 cycles. Any discontinuity between the pellet and the tubing is not revealed.

Local characterisation

The initial porosity of the fuel, controlled in the actual manufacturing way by a pore former addition to the powder, evoluate then as burn-up proceeds, according to the fission gas thermal activated migration, the irradiation induced resintering or the athermal rim build-up mechanisms. The influence of porosity on the material elastic properties is well known. It can be estimated from the variation of the Rayleigh velocity. The study by acoustic microscopy has been conducted by EDF and the Montpellier University on non-irradiated UO_2 samples with calibrated porosity and manufactured by the CEA Grenoble. It has shown that the Rayleigh velocity decreases according to a linear law with increasing porosity, for porosity level not higher than 10%, corresponding to standard as-fabricated pellets :

$$V_R = 2565\ (1 - 0.67p) \qquad (15)$$

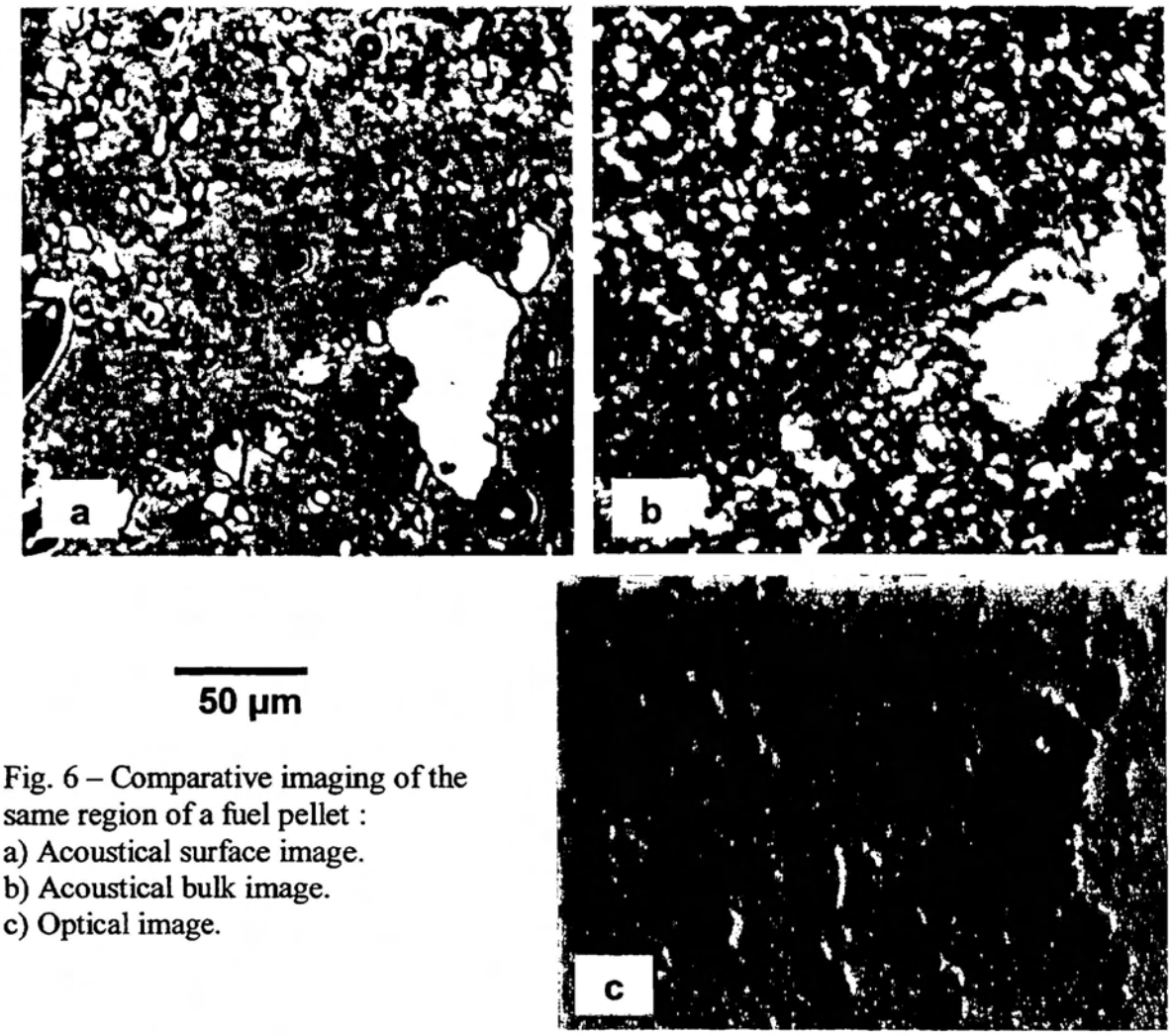

Fig. 6 – Comparative imaging of the same region of a fuel pellet :
a) Acoustical surface image.
b) Acoustical bulk image.
c) Optical image.

The evolution of V_R expected for higher porosity content is estimated (fig. 7) using the models proposed in the open literature to describe the variation of the elastic properties as a function of porosity [12,13] and applying them to the Rayleigh velocity. From these results, the part of each one of the various parameters in the elastic properties can be separated. If the porosity is known, its part on the mechanical properties can be removed, to evaluate the part of the other factors, like the formation of solid solutions with the fission products (fig. 7), the alteration of the anionic sub-lattice or the emergence of non-miscible secondary phases. At the opposite, if the intrinsic elastic properties of the material are known, the porosity can be determined.

In agreement with previous results [14], any influence of the grain size on the Rayleigh velocity has not been observed. The elastic constants being calculated through the knowledge of the velocity of 2 modes of acoustic waves, the longitudinal velocity V_L is provided by microechography measurements. The shear velocity V_T is deduced from V_L and V_R through the relation (5). The mechanical features, Young modulus E, shear modulus G (fig. 8) and Poisson's coefficient ν can be calculated from the measurement of V_L and V_T and from the knowledge of the density ρ by the relations (2-4).

The measure of the Rayleigh velocity having be revealed a suitable parameter to characterise the alteration of the mechanical properties of the nuclear fuels, a profile of V_R

along the radius of an irradiated pellet has been carried out (fig. 9). The very low value of V_R in the rim zone agrees with its high porosity.

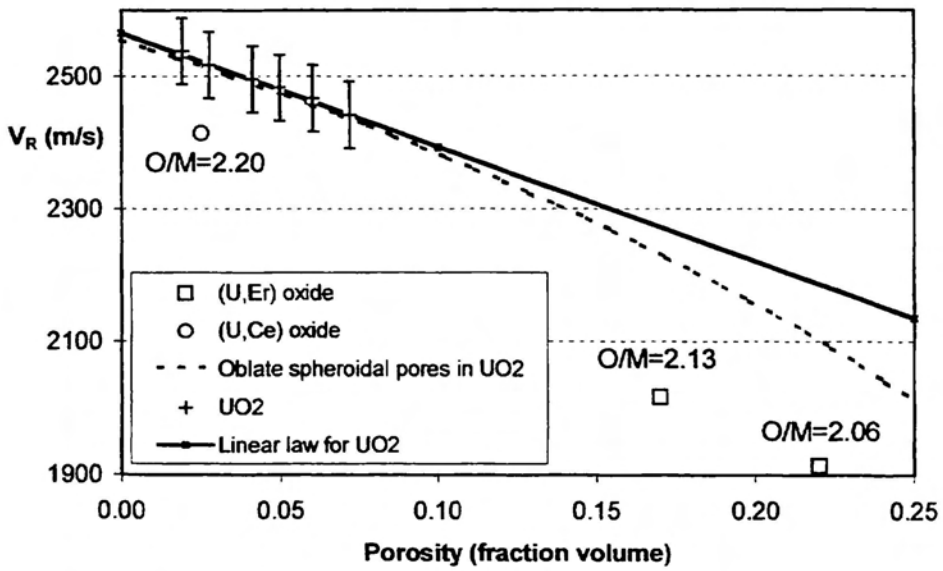

Fig. 7 – Variation of the Rayleigh velocity V_R in uranium dioxide UO_2 as a function of the porosity calculated, from our results, according to : ——— a linear law of evolution; - - - the Berryman model on the assumption of spherical pores. The shift of velocity in $(U_{1-y}Ln_y)O_{2+x}$ solid solutions of lanthanoid elements is marked by o for Ln = Ce and □ for Ln = Er (O/M = 2+x is the oxygen/metal ratio).

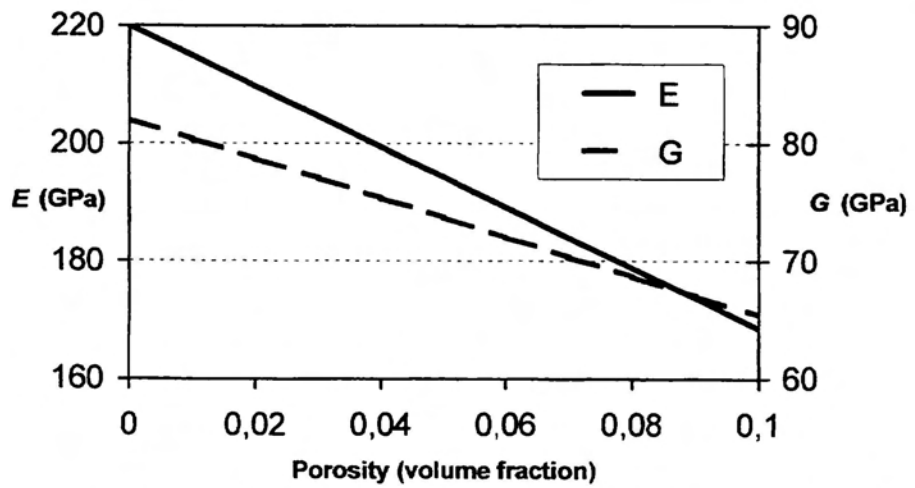

Fig. 8 – Variation of the elastic modulus E and G as a function of the porosity of uranium dioxide UO_2 calculated through the acoustic wave velocity measurements.

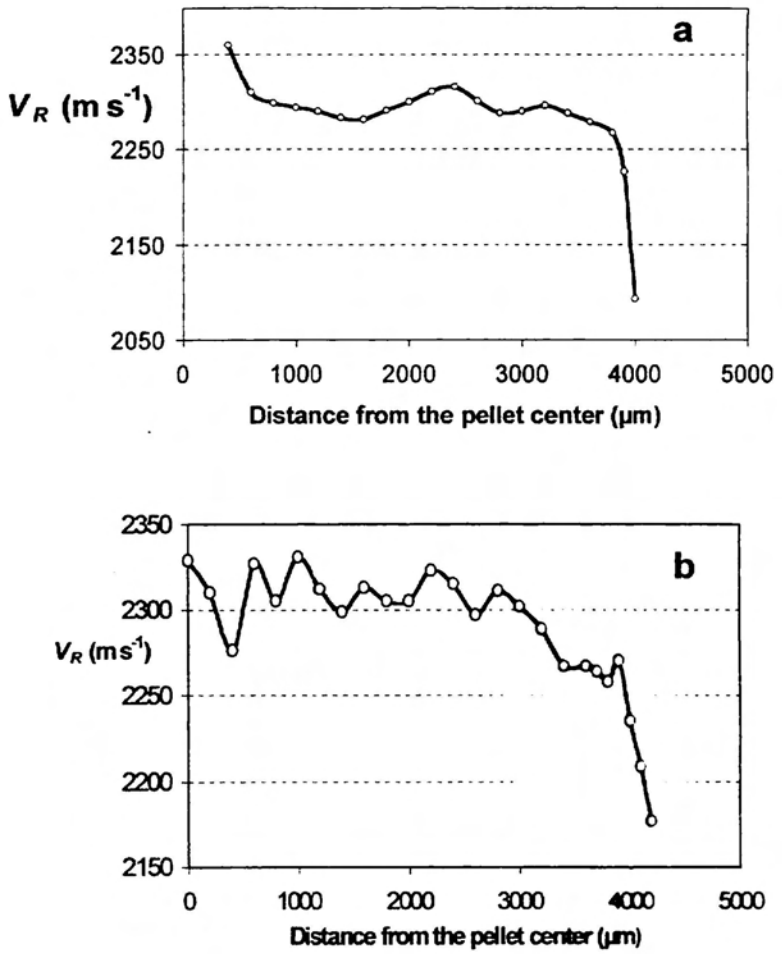

Fig. 9 – Profile of the Rayleigh velocity V_R along a radius of a 2 cycles (a) and a 5 cycle (b) fuel pellet.

DISCUSSION AND CONCLUSION

The microacoustic techniques, acoustic microscopy and microechography provide measurements of the Rayleigh velocity and the longitudinal velocity, from which the elastic constant can be deduced. Correlation have been presented with the material porosity. These measurements are local enough to be carried out on pellet fragments or to characterise the properties variation along a pellet radius. The choice of the acoustic wave length depends on the heterogeneity scale of the material investigated. This wavelength must be much larger than the heterogeneity size, to avoid a too important mitigation of the signal. Accounting for the initial fuel material porosity spectrum (1 to 40 µm), the 15 MHz low frequency technique has been developed to make easier the first studies in hot cell. Nevertheless to characterise the rim zone, typically 100 to 200 µm wide, higher frequencies should be developed to improve measurement resolution. In this way, a 130 MHz acoustic sensor has been designed. Moreover, studies on couplants with acoustic properties better adapted to the samples characteristics are in progress.

Obviously, the elastic properties depend on the porosity, additives, irradiation damage and the presence of secondary phases. Works are still going on to discriminate this different influences.

These original techniques will then be a potential methods in the characterisation of irradiated materials and will provide with an alternative method to evaluate the local porosity volume. Nevertheless, this is only one application of a technical field which have already shown during the feasibility phase many other promising possible use on the entire fuel rod characterisation. For example, it can be adapted for non-destructive mechanical testing of the cladding, in measuring the gap width before a power ramp or the corrosion layer thickness on the inner or outer faces of the cladding, in characterising the local hydrides concentration through the claddings, in characterising the nature of the contact between the fuel pellet and the cladding or the real bonding of the corrosion layer (Zirconia spalling) ... A non destructive gas pressure measurement has already been developed for nuclear fuel rods [15].

Acknowledgements

The authors acknowledge gratefully Josselyne Bourgoin who was at the origin of the idea and also Philippe Dehaudt from the CEA Grenoble who provided the project with characterised samples and with theoretical interpretations.

BIBLIOGRAPHY

1. J. SPINO, K. VENNIX, M. COQUERELLE, J. Nucl. Mater. 231, 179 (1996)
2. J. SPINO, D. BARON, M. COQUERELLE, A.D. STALIOS, "High burn-up rim structure: evidences that xenon-depletion, pore formation and grain subdivision start at different local burn-ups", J. Nucl. Mater., 256, 189-196 (1998)
3. R. MANZEL, R. EBERLE, in : Proc. Int. Topical Meeting on LWR Fuel Performance, Avignon, France, p. 528 (1991)
4. P.G. LUCUTA, Hj. MATZKE, I. HASTINGS, J. Nucl. Mater., 232, 166, (1996)
5. R. MANZEL, M. COQUERELLE, in : Proc. Int. Topical Meeting on Light Water Reactor Fuel Performance, Portland, Oregon, p. 463 (1997)
6. O.L. ANDERSON, "A simplified method for calculating the Debye temperature from Elastic Constants", J. Phys. Solids, 24, 909-917 (1963)
7. I.J. FRITZ, "Elastic properties of UO_2 at high pressure", J. Appl. Phys., 47, 10 76
8. A. BRIGGS, "Acoustic Microscopy", Clarendon, Oxford (1992)
9. R.J.M. DA FONSECA, L. FERDJ-ALLAH, G. DESPAUX, A. BOUDOUR, L. ROBERT, J. ATTAL, "Scanning acoustic microscopy – Recent applications in materials science", Adv. Mater., 7/8, 508-519 (1993)
10. B. CROS, V. GIGOT, G. DESPAUX, "Study of the efficiency of coupling fluids for acoustic microscopy", Appl. Surf. Sci., 119, 242-252 (1997)
11. V. ROQUE, D. BARON, J. BOURGOIN, J.M. SAUREL, "Study by acoustic microscopy of irradiated and non irradiated uranium dioxide", J. Nuclear Mater. (1999), in the press
12. D.G. MARTIN, "The Elastic Constants of polycristalline UO_2 and (U, Pu) mixed oxides : a review and recommendations", High Temperature-High Pressure, 21, 13-24 (1989)
13. J.G. BERRYMAN, Long-wavelength propagation in composite elastic media. I. Spherical inclusions, J. Acoust. Soc. Am., 68, 1809-1819 (1980)
14. N. IGATA, K. DOMOTO, "Fracture stress and elastic modulus of uranium dioxide including excess oxygen", J. Nuclear Mater., 45, 317-322 (1972)
15. M.F. NARBEY, D. BARJON, G. DESPAUX, "Acoustic method to determine the composition of gas mixture such as He-Xe in zircalloy claddings containing the nuclear fuel in PWRs", to be published